Title
INFLUENCE OF EXOTHERMICITY ON THE SHAPE OF A DIFFUSION FLAME

Authors
Klajn, M.
Oppenheim, A.K.

Publication Date
1981-12-01

LBL-13673

Lawrence Berkeley Laboratory
UNIVERSITY OF CALIFORNIA

ENERGY & ENVIRONMENT
DIVISION

Submitted for presentation at the 19th International Symposium on Combustion, Haifa, Israel, August 8-13, 1982

INFLUENCE OF EXOTHERMICITY ON THE SHAPE OF A DIFFUSION FLAME

M. Klajn, and A.K. Oppenheim

December 1981

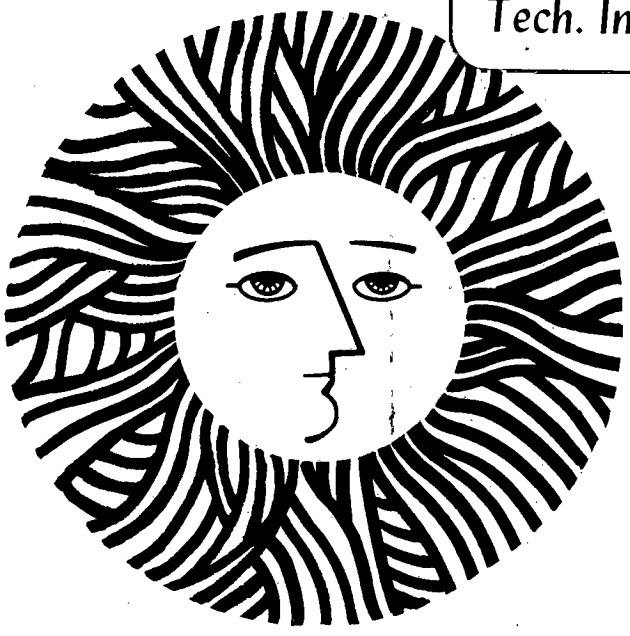

Prepared for the U.S. Department of Energy under Contract W-7405-ENG-48

DISCLAIMER

Submitted for presentation at the 19th International Symposium on Combustion

August 8-13, 1982

Haifa, Israel

INFLUENCE OF EXOTHERMICITY ON THE SHAPE OF A DIFFUSION FLAME

M. Klajn, IIT-Technion, Haifa, Israel

and

A. K. Oppenheim, Lawrence Berkeley Laboratory,
University of California
Mechanical Engineering Department
Berkeley, CA 94720

This work was supported by the Office of Energy Research, Office of Basic Energy Sciences, Division of Basic Engineering Research of the Department of Energy under Contract W-7405-ENG-48, National Science Foundation under Grant ENG 78-12372, and the NASA Lewis Research Center under Grant NAG 3-131.

ABSTRACT

The effects of exothermicity of combustion on the contours of gaseous, unconfined, planar and axi-symmetric, jet diffusion flames, as well as on the structures of their flow fields, are analyzed. For the sake of clarity, the problem is formulated in the simplest possible way. The flame is treated as essentially laminar, the reaction rates are considered infinite, the medium is assumed to behave as a perfect gas with constant specific heats, its Schmidt and Prandtl numbers being unity and viscosity proportional to the temperature, while the buoyancy effects are neglected. Under such circumstances the problem lends itself to treatment by the Shvab-Zeldovich technique. The results, derived as an inverse to self-similar solutions in the incompressible domain obtained by a Dorodnitsyn-Howarth transformation of the governing equations for compressible flow, are expressed in terms of algebraic formulae. In applications to hydrogen-air and a number of hydrocarbon-air mixtures, they turn out to be in an amazing agreement with experimental data under zero gravity conditions.

INTRODUCTION

The explicit purpose of our study was to determine specifically the effect of exothermicity due to combustion on the shape of a gaseous jet diffusion flame.

The subject of our interest has a rich scientific background, having been based on the classical papers of Burke and Schumann [1], Hottel and Hawthorne [2], Wohl, Gazley and Knapp [3], Shvab [4], and Zeldovich [5], while currently it is of particular interest in connection with fire research, as reviewed recently in a comprehensive manner by Pagni [6]. Of special relevance to the theory we developed are the publications of Abramovich [7], Vulis [8], Fay [9], and Goldburg and Cheng [10], while, with respect to its subject matter, are the NASA reports of Edelman, Fortune and Weilrstrein [11], Cochran [12], and Haggard and Cochran [13] concerned with the effects of gravity on laminar diffusion flames.

In all these publications, however, the problems subjected to analysis were formulated in such a way that the exothermic effects of combustion were either of negligible significance or they were buried among others, obliterating their actual influence. It is then for this reason that our study was undertaken.

FORMULATION

For the sake of clarity and simplicity, our theory is cast within a formidable set of idealizations, namely:

1. the flame is laminar, being established in an essentially viscous flow field.

2. the reaction rates are infinite so that the flame front is infinitely thin

3. the flowing substance behaves as a perfect gas with constant specific heats

4. the Schmidt and Prandtl numbers, and hence the Lewis number, are all equal to one

5. the coefficient of viscosity is directly proportional to absolute temperature

6. the effects of buoyancy are neglected, so that the analysis applies to an effectively gravitationless environment

7. the fuel jet has initially a plug flow velocity profile

Under such circumstances, the flow field of a diffusion flame at an essentially uniform pressure can be described in terms of the continuity equation

$$\frac{\partial}{\partial z}\left(\frac{r^j}{\gamma} W\right) + \frac{\partial}{\partial r}\left(\frac{r^j}{\gamma} V\right) = 0 \tag{1}$$

and the equation of motion

$$\frac{r^j}{\gamma} W \frac{\partial W}{\partial z} + \frac{r^j}{\gamma} V \frac{\partial W}{\partial z} = \frac{1}{Re_i} \frac{\partial}{\partial r}\left(\mu r^j \frac{\partial W}{\partial r}\right) \tag{2}$$

In the above z and r are the axial and radial space coordinates respectively, W and V are the corresponding components of the flow velocity vector, ν is the specific volume, and μ is the coefficient of viscosity, all normalized with respect to their initial values, Re_i is the initial Reynolds number based on the radius, while the index j is equal to 0 for planar and 1 for axi-symmetric flow.

As a consequence of our idealizations, all the transport equations, that is the equations of the conservation of species and energy, can be expressed in a form identical to (2) by the introduction of the Shvab-Zeldovich [5] transport variable [4]

$$\beta \equiv \frac{b}{b_i}$$

subscript i denoting the initial values, while $b = b_{\tau k}$ (k = 1, 2, 3), or b_{12}, or b_{13}, or b_{23}, where $b_{12} = b_{\tau 1} - b_{\tau 2}$ etc. Here

$$b_{\tau k} = a\tau + \alpha_k$$

while $a \equiv c_p(T_F - T_i)/fq = (y_{2\infty}^{-1} + f)^{-1}$ where c_p is the specific heat at constant pressure, T_F is the adiabatic flame temperature, f is the mass ratio of fuel initially in the jet and the corresponding stoichiometric amont of oxygen, and q is the specific exothermic energy or the heat of combustion per unit mass, $\tau \equiv (T - T_i)/(T_F - T_i)$, and $\alpha_k = y_1/f$, or $= y_2 - y_{2\infty}$, or $= -y_3/(f+1)$, depending on whether k = 1 (for fuel), k = 2 (for oxygen), or k = 3 (for oxygenated products).

One has therefore six equations of the form identical to (2) where the velocity gradient is replaced by the gradient of the appropriate transport variable. The Shvab-Zeldovich technique we employed for this purpose is described in Appendix A, while its consequences, associated with the fact that at the flame front $y_1 = f y_2$, or $y_1 = 0$ and $y_2 = 0$, while $\tau = 1$, are presented in Table 1, where subscript F denotes conditions at the flame front. The normalized specific volume

at the flame front, γ_F, and the normalized flow velocity at the flame front, w_F, are constants for a given fuel. Their values for hydrogen and for a number of hydrocarbons are listed, together with their other relevant properties, in Table 2.

Our problem involves thus the solution of Eqs. (1) and (2), subject to the following initial and boundary conditions:

@ $z = 0$

$r \leq 1$: $\quad w = \beta = y_1 = 1 \qquad \frac{\partial w}{\partial r} = v = \tau = y_2 = y_3 = 0$

$r > 1$: $\quad y_2 = y_{2\infty} \qquad w = \beta = \tau = y_1 = y_3 = 0$

@ $z > 0$

$r = \pm\infty$: $\quad y_2 = y_{2\infty} \qquad w = \beta = \tau = y_1 = y_3 = 0$

$r = 0$: $\quad \frac{\partial w}{\partial r} = \frac{\partial \beta}{\partial r} = 0$

SOLUTION

Dorodnitsyn-Howarth Transformation

The awkward effects of density variation are first eliminated by the use of the Dorodnitsyn-[14] Howarth [15] transformation. This is executed by the introduction of the following variables:

$$\tilde{z} = z \qquad \tilde{r}^{j+1} = \int_0^r \frac{1}{\nu} dr^{j+1}$$

and

$$\tilde{w} = w \qquad \tilde{v} = \xi^j \left(\frac{v}{\nu} + \frac{w}{rj} \frac{\partial}{\partial r} \int_0^r \frac{r^j}{\nu} dr \right)$$

where

$$\xi \equiv \frac{r}{\tilde{r}}$$

Equations (1) and (2) become then, respectively,

$$\frac{\partial}{\partial \tilde{z}} (\tilde{r}^j \tilde{w}) + \frac{\partial}{\partial \tilde{r}} (\tilde{r}^j \tilde{v}) = 0 \tag{3}$$

and

$$\tilde{r}^j \tilde{w} \frac{\partial \tilde{w}}{\partial \tilde{z}} + \tilde{r}^j \tilde{v} \frac{\partial \tilde{w}}{\partial \tilde{r}} = \frac{1}{Re_i} \left(\frac{\mu}{\nu} \xi^{2j} \tilde{r}^j \frac{\partial \tilde{w}}{\partial \tilde{r}} \right) \tag{4}$$

while the initial and boundary conditions are

@ $\tilde{z} = 0$

$\tilde{r} \leq 1$: $\tilde{w} = 1$ $\qquad \frac{\partial \tilde{w}}{\partial \tilde{r}} = \tilde{v} = 0$

$\tilde{r} > 1$: $\tilde{w} = 0$

@ $\tilde{z} > 0$

$\tilde{r} = \pm \infty$: $\tilde{w} = 0$; $\tilde{r} = 0$: $\partial \tilde{w} / \partial \tilde{r} = 0$

It should be noted that the specific volume is completely eliminated if, as specified at the outset, one has $\mu = \nu$. Since for the planar case $j = 0$, Eq. (4) is independent of ξ and the situation is straightforward. This is not so, however, in the axi-symmetric case, a circumstance that led to the belief that there is no solution in this case, as succinctly stated by Goldburg and Cheng [10] when they wrote: "a complete analytical solution of the cylindrical

laminar jet of varying density does not exist."* Although we are not denying the absolute truth of this statement, we wish to show that there exists not only a possibility of obtaining a set of particular solutions, but also they lend themselves to a most satisfactory approximation which can be expressed in a closed algebraic form, demonstrating with great clarity the role played by exothermicity -- the prime objective of our study. It is, in fact, this aspect of our work that may be regarded as one of its most interesting features.

---

* viz. ref (10), p. 268

Momentum Integral Equation

If (3), multiplied by $\tilde{W}$, is added to (4), the resulting expression can be integrated immediately, yielding the momentum integral equation:

$$\frac{\partial}{\partial \tilde{z}} \int_0^{\tilde{r}_*} \tilde{r}^j \tilde{W}^2 \, d\tilde{r} + \tilde{r}_*^j \tilde{V}_* \tilde{W}_* = \frac{1}{Re_i} \xi^{2j} \tilde{r}_*^j \left| \frac{\partial \tilde{W}}{\partial \tilde{r}} \right|_{\tilde{r}_*} \tag{5}$$

where the variables at the upper limit of integration are denoted by an asterisk subscript, while, it should be recalled, at $\tilde{z} = 0$, $\tilde{V} = 0$ and $\partial \tilde{W} / \partial \tilde{r} = 0$, as a consequence of the last idealization on our list. Moreover, since by virtue of the initial conditions at $\tilde{z} = 0$ one has there also, for $\tilde{r} \leq 1$, $\tilde{W} = 1$, while, for $\tilde{r} > 1$, $\tilde{W} = 0$, Eq. (5) for $\tilde{r}_* = \infty$ yields the momentum integral constant in the following form:

$$\int_0^{\infty} \tilde{r}^j \tilde{W}^2 \, d\tilde{r} = \left| \tilde{W}^2 \frac{\tilde{r}^{j+1}}{j+1} \right|_{\tilde{W} = \tilde{r} = 1} = \frac{1}{j+1} \tag{6}$$

Self-Similar Solution

In the spirit of the boundary layer theory, let

$$\tilde{W}(\tilde{z},\tilde{r}) = \tilde{W}_{\ell}(\tilde{z})\, f(\eta)$$

where

$$\eta \equiv \tilde{r}/\tilde{\delta} \quad , \quad \tilde{\delta} = \tilde{\delta}(\tilde{z}) \, ,$$

The momentum integral equation yields then for $\tilde{r}_* = \infty$

where
$$\left.\begin{aligned} \int_0^{\infty} \tilde{r}^j \tilde{W}^2 \, d\tilde{r} &= \frac{\tilde{W}^2 \tilde{\delta}^{j+1}}{j+1} F \\ F &\equiv \int_0^{\infty} f^2(\eta)\, d\eta^{j+1} \end{aligned}\right\} \qquad (7)$$

In view of (6) this yields immediately a direct relationship between the center line velocity, W_{ℓ}, and the half-width of the jet, $\tilde{\delta}$, namely

$$\tilde{W}_{\ell}^2 \, \tilde{\delta}^{j+1} = F^{-1} \qquad (8)$$

and, as demonstrated in Appendix B, the momentum integral equation is reduced to the following relatively simple form, an equation governing the decay of the center line velocity,

where
$$\left.\begin{aligned} \tilde{W}_{\ell}^{-\frac{4}{j+1}} \frac{d\tilde{W}_{\ell}}{d\tilde{z}} &= \frac{G}{Re_i} \tilde{S}_*^{2j} \\ G &\equiv F^{\frac{2}{j+1}} \frac{\eta_*^j}{f(\eta_*)\int_0^{\eta_*} f(\eta)\, d\eta} \left|\frac{df(\eta)}{d\eta}\right|_{\eta_*} \end{aligned}\right\} \qquad (9)$$

As one should expect, a significant simplification is obtained by adopting for $f(\eta)$ the Schlichting solution for a laminar jet [16], namely

$$f(\eta) = \begin{cases} 1 - \tanh^2 \eta & \text{for } j=0 \\ \dfrac{1}{(1+\eta^2)^2} & \text{for } j=1 \end{cases} \tag{10}$$

In both cases the functions F and G are reduced to constants which can be expressed comprehensively as follows:

$$F = \frac{2^{j+1}}{3} \quad ; \quad G = -\frac{8}{3^{2-j}} \tag{11}$$

The governing equations (9) and (8) yield then, respectively, the following straightforward expressions:

$$\tilde{W}_\ell - \frac{4}{j+1} \frac{d\tilde{W}_\ell}{d\tilde{z}} = -\frac{8}{3^{2-j} Re_i} \tilde{\xi}_*^{2j} \tag{12}$$

and

$$\tilde{\delta}^{j+1} = \frac{3}{2^{j+1} \tilde{W}_\ell^2} \tag{13}$$

Planar Flame ($j = 0$)

In this case $\xi^{2j} = 1$, so that Eq. (12) can be integrated immediately. Noting that, according to the Dorodnitsyn-Howarth transformation, $\tilde{z} = z$ and $\tilde{w} = w$, one obtains thus

$$\boxed{w_\ell = \left(1 + \frac{8}{3}\frac{\hat{z}}{Re_i}\right)^{-\frac{1}{3}}} \tag{14}$$

where $\hat{z} = z - z_o$ denotes the coordinate of the jet corresponding to self-similar solution in the transformed plane.

Since at the flame tip $w_\ell = w_F$, flame height is hence given by

$$\frac{\hat{z}_F}{Re_i} = \frac{3}{8}\left(w_F^{-3} - 1\right) \tag{15}$$

a constant for a given fuel independent of ν, i.e. unaffected by the exothermicity of the combustion process.

In order to evaluate the radial coordinate of the flame front, the Dorodnitsyn-Howarth transformation has to be inversed:

This involves the quadrature

$$r = \int_0^{\tilde{r}} \nu \, d\tilde{r}$$

where, as a consequence of the Shvab-Zeldovich technique (viz. Table 1),

$$\nu = \frac{\nu_F - w_F}{1 - w_F} - \frac{\nu_F - 1}{1 - w_F}\tilde{w}$$

In terms of the Schlichting solution for $j = 0$

$$\tilde{w} = \tilde{w}_\ell(\tilde{z})\left(1 - \tanh^2 \eta\right)$$

while $\tilde{r} = \tilde{\delta}\eta$, where, according to (13),

$$\tilde{\delta} = \frac{3}{2\tilde{W}_{\ell}^{2}}$$

remains constant in the process of quadrature. Noting finally that, as a particular consequence of the above Schlichting solution,

$$\tanh \eta_F = \sqrt{1 - \frac{W_E}{\tilde{W}_{\ell}}}$$

while $\tilde{W} = W$, the inverse transform yields

$$\boxed{r_F = \frac{3}{2(1-W_F)W_{\ell}^{2}}\left[(\nu_F - W_F)\operatorname{arctanh}\sqrt{1-\frac{W_E}{W_{\ell}}} - (\nu_F - 1)W_{\ell}\sqrt{1-\frac{W_E}{W_{\ell}}}\right]} \qquad (16)$$

completing the solution. The shape of the flame front is obtained by evaluating W_{ℓ} from (14) and then r_f from (16).

Typical results are depicted in Fig. 1. Shown on the right is a typical case of a hydrocarbon for which, as indicated in Table 2, $W_F = 0.06$. On the left are corresponding results obtained for a diluted fuel, for which the fuel/oxygen ratio, f, is larger (viz. Eq. (A.9)). The corresponding values of ν_F are modified in order to satisfy the fuel dilution invariant, Eq. (A .10). In both cases the flame height is not affected by the exothermic effects expressed in terms of ν_F.

Axi-Symmetric Flame ($j = 1$)

Here $\xi^{2j} = \xi^2 > 1$, and the inverse Dorodnitsyn-Howarth transformation is required even for the evaluation of the axial coordinate of the flame. This involves now the following integration

$$r^2 = \int_0^{\tilde{r}^2} \nu \, d\tilde{r}^2 = \int_0^{\tilde{r}^2} \left(\frac{\nu_E - W_E}{1 - W_E} - \frac{\nu_E - 1}{1 - W_E} \tilde{W} \right) d\tilde{r}^2 = \frac{\nu_E - W_E}{1 - W_E} \tilde{r}^2 - \frac{\nu_E - 1}{1 - W_E} W_\ell \tilde{\delta}^2 \int_0^{\eta^2} f(\eta) \, d\eta^2 \qquad (17)$$

Since in this case the Schlichting solution is

$$f(\eta) = \frac{1}{(1+\eta^2)^2}$$

it follows that

$$\int_0^{\eta^2} f(\eta) \, d\eta^2 = \frac{\eta^2}{1+\eta^2}$$

and, noting that $\tilde{\delta}^2 \eta^2 = \tilde{r}^2$, Eq. (17) yields the following expression for the dilation factor

$$\xi^2 \equiv \frac{r^2}{\tilde{r}^2} = \frac{\nu_E - W_E}{1 - W_E} - \frac{\nu_E - 1}{1 - W_E} \frac{W_\ell}{1+\eta^2} \qquad (18)$$

Now, in order to evaluate the axial coordinate, Eq. (12) has to be integrated for a set of intermediate values of $\eta = \eta_*$ using (18). The flame height is then obtained for $W_\ell = W_F$ as a function of η_*. The algebra is somewhat involved and for this reason its details have been delegated here to Appendix C. The results, presented in Fig. 2, demonstrate that, irrespectively of the value of ν_F expressing the extent of exothermicity, the flame height, $\hat{z}_F$, is quite insensitive to the particular choice of η_*, remaining at a remarkably constant level for $0 < \eta_* < 0.8$, while the axial flow velocity, whose variation is displayed by $f(\eta)$, falls down to as much as one third of its value at the center line.

This suggested to us that a very good approximation can be obtained by assuming in (18) $\eta^2 = 0$, so that ξ^2 becomes a straightforward linear function of W_ℓ. Under such circumstances the situation is vastly simplified and Eq. (12) can be integrated without much ado,

yielding

$$\boxed{\frac{\hat{Z}}{Re_i} = \frac{3}{8}\frac{1-W_E}{\gamma_E-W_E}\left[\frac{1-W_\ell}{W_\ell} + \frac{\gamma_E-1}{\gamma_E-W_E}\ln\frac{\gamma_E-W_E+(1-\gamma_E)W_\ell}{(1-W_E)W_\ell}\right]} \tag{19}$$

whence the flame height, corresponding to $W_\ell = W_E$, is given by

$$\frac{\hat{Z}_E}{Re_i} = \frac{3}{8}\frac{1-W_E}{\gamma_E-W_E}\left[\frac{1-W_E}{W_E} + \frac{\gamma_E-1}{\gamma_E-W_E}\ln\frac{\gamma_E}{W_E}\right] \tag{20}$$

The evaluation of the flame radius is now particularly simple. Noting that

$$r_E = \left(\frac{r_E}{\tilde{r}_E}\right)\tilde{r}_E = \Xi_E\,\eta_E\,\tilde{\delta}$$

while, according to the Schlichting solution for $j = 1$,

$$\eta_E^2 = \sqrt{\frac{W_\ell}{W_E} - 1}$$

and, by virtue of (13),

$$\tilde{\delta}^2 = \frac{3}{4W_\ell^2}$$

whereas from Eq. (18)

$$\Xi_E^2 = \frac{\gamma_E - W_E}{1-W_E} - \frac{\gamma_E-1}{1-W_E}\frac{W_\ell}{1+\eta_E^2}$$

one obtains immediately

$$\boxed{r_E^2 = \frac{3}{4W_E^2}\left(\frac{W_E}{W_\ell}\right)^2\left(\sqrt{\frac{W_\ell}{W_E}} - 1\right)\left(\frac{\gamma_E-W_E}{1-W_E} - \frac{\gamma_E-1}{1-W_E}W_E\sqrt{\frac{W_\ell}{W_E}}\right)} \tag{21}$$

As before, the flame shape is expressed in an algebraic form, now Eqs. (19) and (21), with the center line velocity, W_ℓ, as a parameter.

To complete the solution, we obtained a very simple expression for maximum flame width by noting that it occurs when

$$W_\ell \approx \frac{16}{9} W_F$$

corresponding to the condition $d r_F^2/dz = 0$ evaluated from Eqs. (19) and (21). The latter yields then the following expression for the maximum flame width

$$r_{F_{max}} \approx \frac{9}{32} \frac{\sqrt{\nu_E}}{W_F} \left(1 - \frac{2}{3} W_F\right) \approx 0.27 \frac{\sqrt{\nu_E}}{W_F}$$

while the former, combined with Eq. (20), specifies its location as

$$\hat{z}_{r_{F_{max}}} \approx 0.6\, \hat{z}_F$$

in excellent agreement with results of numerical computations of Edelman et al. [11].

RESULTS AND CONCLUSIONS

In contrast to the case of planar flames presented in Fig. 1, the height of axi-symmetric flames is distinctly dependent on the exothermic effects expressed in terms of ν_F as depicted in Fig. 3. The diagram shows also the remarkable similarity between the results obtained for $\eta^* = 0.8$ by the method described in Appendix C, and those of Eqs. (19) and (21), demonstrating the excellence of the approximation they provide.

Figure 4 presents the axial velocity profiles in the axi-symmetric case when $\nu_F = 7$ and $\mu_F = 0.06$. For the sake of clarity they are here normalized with respect to the center line velocity, while the corresponding radius is normalized with respect to its value at a section where the axial velocity is one quarter of its maximum at the center. Vertical dashes at each profile denote the position of the flame. The graph demonstrates clearly that the velocity profile of the flow field around a diffusion flame is definitely not self-similar, as pointed out by Hottel and Hawthorne [2]. However, our results are based on a self-similar solution on the transformed plane.

The corresponding flame structures at its initial section and at one tenth of its height are shown in Fig. 5. They are described in terms of the axial velocity profiles denoted by w, the specific volume, η, representing in effect the temperature variation, and the concentrations of fuel, oxygen and oxygenated products marked respectively by y_1, y_2, and y_3.

The heights of axially symmetric flames evaluated from our theory are compared in Fig. 6 to experimental results measured under zero-gravity conditions by Cochran [12] and Haggard and Cochran [13]. With the exception of propylene, the agreement is indeed amazing, taking especially into account the formidable extent of idealizations on which our solution is based. The corresponding comparison of maximum flame widths is depicted in Fig. 7. Our solution

is independent of the flow rate, while the experimentally observed variation seems to occur primarily at low flow rates tending towards assymptotes in fair agreement with our theory. In view of the intrinsic difficulties in experimental measurements, this agreement should be considered as quite satisfactory.

To sum up, we have derived analytic solutions for planar and axi-symmetric gaseous jet diffusion flames. Our results are expressed in terms of straightforward algebraic expressions where the influence of exothermicity is clearly evident. They are shown to be in good agreement with experimental data obtained under zero gravity conditions to which, for the sake of clarity and simplicity, our theory has been restricted. In doing this we have obviated,by means of a most satisfactory approximation, an essential difficulty registered clearly in the literature, undoubtedly the principal reason why the solution we present here has not been obtained before.

REFERENCES

1. Burke, S. P., and Schumann, T. E. W.: "Diffusion Flames" First Symposium on Combustion, pp. 2-11, Swampsott, Mass., 1928 (Reprint of Proceedings published by The Combustion Institute in 1965; viz. also Ind. Engg. Chemistry, 20, 998-1009, 1928).

2. Hottel, H. C., and Hawthorne, W. R.: "Diffusion in Laminar Flame Jets" Third Symposium on Combustion and Flame and Explosion Phenomena, 254-266, The Williams and Wilkins Company, Baltimore, Maryland, 1949.

3. Wohl, K., Gazley, C., and Kapp, N.: "Diffusion Flames" Third Symposium on Combustion and Flame and Explosion Phenomena, 288-300, The Williams and Wilkins Company, Baltimore, Maryland, 1949.

4. Shvab, V. A.: "Relationship Between the Temperature and the Velocity Field of a Gaseous Flame (Zviaz Miezdy Temperaturnymi i Skoroştnymi Poliami Gazovoyo Fakiela) Zh. T.F. (Journal of Technical Physics, 11, 5, 431-442, 1941).

5. Zeldovich, Ya. B.: "On the Theory of Combustion of Initially Unmixed Gases (K Teorii Gorenia Nepereme-Shanykh Gazov) Zh. T.F. (Journal of Technical Physics, 19, 10, 1199-1210, 1949; transl.: N.A.C.A., Tech. Memorandum 1296, 20 pp., 1951).

6. Pagni, P. J.: "Diffusion Flame Analysis" Fire Safety Journal, 3, 273-285, 1980/81.

7. Abramovich, G. N.: The Theory of Turbulent Jets. Transl. MIT Press, Cambridge, Mass., 671 pp., 1963.

8. Vulis, L. A., Ershin, Sh. A., and Yarin, L. P.: Fundamentals of the Theory of a Gaseous Flame (Osnovy Teorii Gazovovo Fakiela) Energia, Lenningraskoie Otdfelenie, 204 pp., 1968.

9. Fay, J. A.: "The Distribution of Concentration and Temperature in a Laminar Jet Diffusion Flame" J. Aero. Sci., 21, 681-689, 1954.

10. Goldburg, A., and Cheng, S. I.: "A Review of the Fluid Dynamic Problem Posed by the Laminar Jet Diffusion Flame" Combustion and Flame, 9, 259-272, 1965.

11. Edelman, R. B., Fortune, O., and Weilrstein, G.: Analytical Study of Gravity Effects on Laminar Diffusion Flames, NASA CR-120921, 136 pp., 1972.

12. Cochran, T. H.: Experimental Investigation of Laminar Gas Jet Diffusion Flames in Zero Gravity, NASA TN D-6523, 26 pp., 1972.

13. Haggard, J. B., and Cochran, T. H.: Hydrogen and Hydrocarbon Diffusion Flames in a Weightless Environment, NASA TN D-7165, 28 pp., 1973.

14. Dorodnitsyn, A. A.: "Boundary Layer in a Compressible Gas" (Pogranichnyi Sloi v Szimaiemom Gazie) P.M.M. (Prikladnaia Matematika i Mechanika) 6, 6, 449-486, 1942.

15. Howarth, L.: "Concerning the Effects of Compressibility on Laminar Boundary Layers and Their Separation" Proc. Roy. Soc., A194, 16-42, 1948.

16. Schlichting, H.: Boundary Layer Theory, Transl. by J. Kestin, McGraw-Hill Book Company, Inc. First English Edition, p. 499 Eq. (23.45) and p. 500 Eq. (23.46), 1955.

APPENDIX A

Reduction of Transport Equations by the Shvab-Zeldovich Technique

The equations of the conservation of species and energy, are, in terms of our variables, respectively, as follows:

$$\frac{r^j}{\psi} W \frac{\partial y_k}{\partial z} + \frac{r^j}{\psi} V \frac{\partial y_k}{\partial r} = \frac{1}{Re_i} \frac{\partial}{\partial r}\left(\frac{\mu r^j}{Sc_k} \frac{\partial y_k}{\partial r}\right) + r^j \omega_k \tag{A.1}$$

$$\frac{r^j}{\psi} W \frac{\partial \tau}{\partial z} + \frac{r^j}{\psi} V \frac{\partial \tau}{\partial r} = \frac{1}{Re_i} \frac{\partial}{\partial r}\left(\frac{\mu r^j}{Pr} \frac{\partial \tau}{\partial r}\right) + r^j \Omega \tag{A.2}$$

where

$$\omega_k \equiv \gamma \dot{M}_k''' \qquad \text{and} \qquad \Omega \equiv \frac{q}{c_p(T_f - T_i)} \omega_1$$

$\dot{M}_k'''$ denoting the mass rate of the generation of species k per unit volume, while Sc and Pr are the Schmidt and Prandtl numbers respectively.

The flame is established at the stoichiometric contour where f gms. of fuel ($k = 1$) react with 1 gm. of oxygen ($k = 2$) producing ($f + 1$) gms. of oxygenated products ($k = 3$) and generating fq calories of exothermic energy ("heat"). One has therefore

$$-\omega_1 / f = -\omega_2 = \omega_3 / (f+1) = a\Omega \tag{A.3}$$

where

$$a \equiv \frac{c_p(T_\infty - T_i)}{fq} = \frac{y_{2\infty}}{1 + f y_{2\infty}} \tag{A.4}$$

the last equation expressing the overall energy balance. Thus,

introducing the Shvab-Zeldovich variable

$$b_{\tau k} \equiv a\tau + \alpha_k$$

where

$$\alpha_k = \begin{cases} y_1/f & \text{for } k=1 \\ y_2 - y_{2\infty} & \text{for } k=2 \\ -y_3/(f+1) & \text{for } k=3 \end{cases} \tag{A.5}$$

one obtains by a linear combination of (A.1) and (A.2) specified by (A.5), assuming $Sc_k = Pr = 1$,

$$\frac{r^j}{y^j} W \frac{\partial \beta}{\partial z} + \frac{r^j}{y^j} V \frac{\partial \beta}{\partial r} = \frac{1}{Re_i} \frac{\partial}{\partial r}\left(\mu r^j \frac{\partial \beta}{\partial r}\right) \tag{A.6}$$

where

$$\beta \equiv \frac{b}{b_i}$$

In the above $b = b_{\tau k}$ (k = 1,2,3), or b_{12}, or b_{13}, or b_{23}, where $b_{12} = b_{\tau 1} - b_{\tau 2}$ etc, while subscript i denotes the respective initial values.

Equation (A.6) is identical to Eq. (2) and in our problem their initial and boundary conditions with respect to the appropriate variables are also identical. Hence, everywhere in the field

$$W = \beta \tag{A.7}$$

Thus, except for the a priori unknown variation of density, the problem is governed by the fluid mechanics, equations (1) and (2), so that, once the velocity field is determined, all the other dependent variables of the problem can be evaluated. The algebraic relationships one can use for this purpose are listed in Table 1. They were obtained as follows. Taking

$$W = \beta_{12} = \frac{b_{\tau 1} - b_{\tau 2}}{b_{\tau 1_i} - b_{\tau 2_i}} = \frac{\alpha_1 - \alpha_2}{\alpha_{1_i} - \alpha_{2_i}}$$

and substituting the appropriate expressions of α_k as per (A.5), it follows that

$$W = \frac{y_i - f y_2 + f y_{2\infty}}{1 + f y_{2\infty}} \tag{A.8}$$

At the flame front $y_1 = f y_2$, as well as $y_1 = 0$ and $y_2 = 0$. One has therefore

$$W_F = \frac{f y_{2\infty}}{1 + f y_{2\infty}} \qquad \text{or} \qquad f y_{2\infty} = \frac{W_F}{1 - W_F} \tag{A.9}$$

In view of the fact that at constant pressure $T_F / T_i = \dot{\gamma}_F$, the above, combined with the energy balance expressed by (A.4), yields

$$\frac{\dot{\gamma}_F - 1}{1 - W_F} = \frac{f y_{2\infty} q}{c_p T_i} \tag{A.10}$$

-- an invariant for a given fuel at a specific initial temperature, irrespectively of its dilution. At the same time, using (A.9) to eliminate $f y_{2\infty}$ from (A.8), one obtains

$$W = (y_i - f y_2)(1 - W_F) + W_F \tag{A.11}$$

Since inside the flame $y_2 = 0$, while outside $y_1 = 0$, the above yields $y_1 = y(w)$ as well as $y_2 = y(w)$, as shown in Table 1.

Similarly, taking

$$w = \beta_{13} = \frac{y_1/f + y_3/(f+1)}{1/f} = y_1 + \frac{f}{f+1} y_3$$

one gets

$$y_3 = \frac{f+1}{f}(w - y_1) \tag{A.12}$$

whereas, taking

$$w = \beta_{\tau 1} = \frac{a\tau + y_1/f}{1/f} = fa\tau + y_1$$

and noting that at the flame front $\tau = 1$ while $y_1 = 0$, so that $fa = w_F$, it follows that

$$\tau = \frac{w}{w_F} - \frac{y_1}{w_F} \tag{A.13}$$

Equations (A.11) and (A.13) provide the expressions for $y_3 = y(w)$ and $\tau = \tau(w)$ presented in Table 1. Finally the variation of γ with w is obtained from that of τ by noting that, for a perfect gas with constant specific heats, one has, in a process at constant pressure,

$$\gamma = 1 + (\gamma_F - 1)\tau \tag{A.14}$$

APPENDIX B

Momentum Integral Equation for a Self-Similar Jet

The task is to perform the integration of

$$\frac{\partial}{\partial \tilde{z}} \int_0^{\tilde{r}_*} \tilde{r}^j \tilde{w}^2 d\tilde{r} + \tilde{r}_*^j \tilde{v}_* \tilde{w}_* = \frac{1}{Re_i} \Xi^{2j} \tilde{r}_*^j \left| \frac{\partial \tilde{w}}{\partial \tilde{r}} \right|_{\tilde{r}_*} \tag{5}$$

subject to the similarity transformation

$$\tilde{w}(\tilde{z}, \tilde{r}) = \tilde{w}_\ell(\tilde{z}) f(\eta)$$

where

$$\eta = \tilde{r}/\tilde{\delta} \quad , \quad \tilde{\delta} = \tilde{\delta}(\tilde{z})$$

This is done term by term as follows:

First Term

$$\frac{\partial}{\partial \tilde{z}} \int_0^{\tilde{r}_*} \tilde{r}^j \tilde{w}^2 d\tilde{r} = \frac{d}{dz} \left[\tilde{w}_\ell^2 \tilde{\delta}^{j+1}(\tilde{z}) \int_0^{\eta_*} f^2(\eta) \eta^j d\eta \right]$$

Since from the total momentum integral for a self-similar jet

$$\tilde{w}_\ell^2 \tilde{\delta}^{j+1} = F^{-1} \quad \text{where} \quad F \equiv \int_0^\infty f^2(\eta) d\eta^{j+1} \tag{8}$$

it follows that

$$\frac{\partial}{\partial \tilde{z}} \int_0^{\tilde{r}_*} \tilde{r}^j \tilde{w}^2 d\tilde{r} = \frac{1}{F} \frac{d}{d\eta} \left(\int_0^{\eta_*} f^2(\eta) \eta^j d\eta \right) \frac{d\eta}{d\tilde{z}} = \frac{1}{F} f^2(\eta_*) \eta_*^j \frac{d\eta}{d\tilde{z}} \tag{B1}$$

Second Term

By virtue of the continuity equation, (1),

$$\tilde{r}_*^j \tilde{V}_* = -\frac{\partial}{\partial \tilde{z}}\left(\int_0^{\tilde{r}_*} \tilde{r}^j \tilde{w}\, d\tilde{r}\right) = -\frac{d}{dz}\left[\tilde{w}_\ell \tilde{\delta}^{j+1}\right]\int_0^{\eta_*} f(\eta)\eta^j d\eta$$

In terms of F this becomes

$$\tilde{r}_*^j \tilde{V}_* = -\frac{1}{F}\frac{d}{d\tilde{z}}\left[\frac{1}{\tilde{w}_\ell}\int_0^{\eta_*} f(\eta)\eta^j d\eta\right] = -\frac{1}{F}\left[\frac{d\tilde{w}_\ell}{d\tilde{z}}\tilde{w}_\ell^{-1}\int_0^{\eta_*} f(\eta)\eta^j d\eta + \tilde{w}_\ell^{-1} f(\eta_*)\eta_*^j \frac{d\eta_*}{d\tilde{z}}\right]$$

whence

$$\tilde{r}_*^j \tilde{V}_* = \tilde{r}_*^j \tilde{V}_* \tilde{w}_\ell f(\eta) = \frac{1}{F\tilde{w}_\ell}\frac{d\tilde{w}_\ell}{d\tilde{z}} f(\eta_*)\int_0^{\eta_*} f(\eta)\eta^j d\eta - \frac{1}{F} f^2(\eta_*)\eta_*^j \frac{d\eta_*}{d\tilde{z}} \qquad \text{(B.2)}$$

where, it should be noted, the last term is identical to the first term and has an opposite sign, causing its cancellation

Third Term

$$\tilde{r}^j \frac{\partial \tilde{w}}{\partial \tilde{r}} = \tilde{r}^j \tilde{w}_\ell \frac{\partial f(\eta)}{\partial \tilde{r}} = \frac{\tilde{r}^j}{\tilde{\delta}}\tilde{w}_\ell \left|\frac{df(\eta)}{d\eta}\right|_{\eta_*} = \tilde{w}_\ell \tilde{\delta}^{j-1}\eta_*^j \left|\frac{df(\eta)}{d\eta}\right|_{\eta_*}$$

where, in view of Eq. (8), $\tilde{\delta}$ can be eliminated yielding

$$\tilde{r}^j \frac{\partial \tilde{w}}{\partial \tilde{r}} = F^{\frac{1-j}{j+1}} \tilde{w}_\ell^{\frac{3-j}{j+1}} \eta_*^j \left|\frac{df(\eta)}{d\eta}\right|_{\eta_*} \qquad \text{(B.3)}$$

Substituting (B.1), (B.2) and (B.3) into (5), one gets thus

$$\frac{1}{F\tilde{w}_\ell}\frac{d\tilde{w}_\ell}{d\tilde{z}} f(\eta_*)\int_0^{\eta_*} f(\eta)\eta^j d\eta = \frac{\xi^{2j}}{Re_i} F^{\frac{1-j}{j+1}} \tilde{w}_\ell^{2\frac{1-j}{j+1}} \eta_*^j \left|\frac{df(\eta)}{d\eta}\right|_{\eta_*}$$

whence

$$\left.\begin{aligned} \tilde{w}^{-\frac{4}{j+1}}\frac{d\tilde{w}_\ell}{d\tilde{z}} &= \frac{G}{Re_i}\xi^{2j} \\ \text{where} \\ G &\equiv F^{\frac{2}{j+1}} \frac{\eta_*^j}{f(\eta_*)\int_0^{\eta_*} f(\eta)d\eta}\left|\frac{df(\eta)}{d\eta}\right|_{\eta_*} \end{aligned}\right\} \qquad (9)$$

APPENDIX C

Centerline Velocity Decay and Flame Height in Axi-Symmetric Case ($j = 1$)

One has to distinguish between here three cases:

(a): $W_\ell > W_F$ while $\tilde{r}_* < \tilde{r}_F$, where the integration is performed inside the flame

(b): $W_\ell > W_F$ while $\tilde{r}_* > \tilde{r}_F$, where the integration crosses the flame, and

(c): $W_\ell < W_F$ while $\tilde{r}_* > \tilde{r}_F$, where the integration is performed outside the flame

The last case is of interest only for the determination of the flow field above the flame; hence it is of no concern to the analysis of the flame shape.

The algebraic manipulations in the execution of the inverse Dorodnitsyn-Howarth transformation are, in each case, as follows:

Case (a)

$$r_*^2 = \int_0^{\tilde{r}^2} \nu \, d\tilde{r}^2 = \int_0^{\tilde{r}^2} \left[1 + \frac{\nu_F - 1}{1 - W_F}(1 - W)\right] d\tilde{r}^2 = \frac{\nu_F - W_F}{1 - W_F}\tilde{r}_*^2 - \frac{\nu_F - 1}{1 - W_F} W_\ell \tilde{\delta}^2 \int_0^{\eta_*^2} f(\eta) \, d\eta^2$$

and since, according to the Schlichting solution,

$$f(\eta) = \frac{1}{(1+\eta^2)^2}$$

one has

$$\int_0^{\eta_*^2} f(\eta) \, d\eta^2 = \frac{\eta_*^2}{1+\eta_*^2}$$

Hence

$$\xi^2 \equiv \frac{r_*^2}{\tilde{r}_*^2} = \frac{\nu_F - W_F}{1 - W_F} - \frac{\nu_F - 1}{1 - W_F} \frac{W_\ell}{1+\eta_*^2} \qquad (C.1)$$

Case (b)

$$\frac{r_*^2}{} = \int_0^{\tilde{r}_F^2} \left[1 + \frac{\gamma_F - 1}{1 - W_F}(1 - W)\right] d\tilde{r}^2 + \int_{\tilde{r}_F^2}^{\tilde{r}_*^2} \left[1 + (\gamma_F - 1)\frac{W}{W_F}\right] d\tilde{r}^2$$

and since as demonstrated in the section on the solution for the axi-symmetric flame,

$$W = \frac{W_\xi}{(1+\eta^2)^2} \qquad \text{while} \qquad \eta_F = \sqrt{\frac{W_\xi}{W_F}} - 1$$

one gets now

$$\xi_*^2 = A\frac{W_\xi}{W_F} + B\sqrt{\frac{W_\xi}{W_F}} + C \qquad (C.2)$$

where

$$A = -\frac{\gamma_F - 1}{1 - W_F}\frac{1}{1+\eta_*^2}\left(\frac{1}{\eta_*^2} + W_F\right)$$

$$B = \frac{2}{\eta_*^2}\frac{\gamma_F - 1}{1 - W_F}$$

$$C = 1 - \frac{\gamma_F - 1}{1 - W_F}\frac{1}{\eta_*^2}$$

Case (c) is in all respects similar to case (a), except for the use of the other expression for $\gamma(W)$ in Table 1. Since, this is of no concern to the flame shape, the prime objective of our study, the explicit algebraic solution is not given here.

Now, the centerline velocity decay is determined by the substitution of (C.1) or (C.2) for ξ^2 in Eq. (12). This leads respectively to the following solutions

Case (a)

$$\frac{d\tilde{z}}{Re_j} = -\frac{3}{8}\frac{dW_\xi}{W_\xi^2\left[\frac{\gamma_F - W_\xi}{1 - W_F} - \frac{\gamma_F - 1}{1 - W_F}\frac{W_\xi}{1+\eta_*^2}\right]}$$

whence, since initially, at $\tilde{z} = 0$, $W_\ell = 1$,

$$\frac{\tilde{z}}{Re_i} = \frac{3}{8}\frac{1-W_F}{\gamma_F - W_F}\left[\frac{1}{W_\ell} - 1 + \frac{\gamma_F - 1}{\gamma_F - W_F}\frac{1}{1+\eta_*^2}\ln\frac{(\gamma_F - W_F)(1+\eta_*^2)/W_\ell - (\gamma_F - 1)}{(\gamma_F - W_F)(1+\eta_*^2) - (\gamma_F - 1)}\right]$$

At $\tilde{r}_* = \tilde{r}_F$ $\quad W_F = W_\ell f(\eta_*)$, so that $W_\ell = W_F(1+\eta_*^2)^2$, and noting that $\tilde{z} = \hat{z}$, one gets in this case

$$\frac{\hat{z}}{Re_i} = \frac{3}{8}\frac{1-W_F}{\gamma_F - W_F}\left[\frac{1}{W_F(1+\eta_*^2)^2} - 1 + \frac{\gamma_F - 1}{\gamma_F - W_F}\frac{1}{1+\eta_*^2}\ln\frac{\frac{\gamma_F - W_F}{W_F(1+\eta_*^2)} - (\gamma_F - 1)}{(\gamma_F - W_F)(1+\eta_*^2) - (\gamma_F - 1)}\right] \qquad (C.3)$$

Case (b)

$$o\,\frac{d\tilde{z}}{Re_i} = -\frac{3}{8}\frac{dW_\ell}{W_\ell^2\left[A\frac{W_\ell}{W_F} + B\sqrt{\frac{W_\ell}{W_F}} + C\right]}$$

whence, since the initial conditions here are: $W_\ell = W_{\ell *}$ at $\tilde{z} = \tilde{z}_*$, it follows that

$$\frac{\tilde{z} - \tilde{z}_*}{Re_i} = \frac{3}{8W_F}\left[\mathcal{F}\left(\frac{W_\ell}{W_F}\right) - \mathcal{F}(1+\eta_*^2)\right] \qquad (C.4)$$

where

$$\mathcal{F}(x) = \frac{2B}{C^2\sqrt{x}} - \frac{1}{Cx} + \frac{1}{2C^2}\left(A - \frac{B^2}{C}\right)\ln\frac{Ax + B\sqrt{x} + C}{x} + \frac{B}{2C^2}\left(3A - \frac{B^2}{C}\right)\frac{1}{D}\ln\frac{2Ax + B - D}{2Ax + B + D}$$

while

$$D \equiv \sqrt{B^2 - 4AC}$$

-- a quantity which is always positive.

The flame height is obtained from the above for $\tilde{z}_\ell = \tilde{z}_F$, so that (C.4) yields

$$\frac{\hat{z}_F}{Re_i} = \frac{3}{8W_F}\left[\mathcal{F}(1) - \mathcal{F}(1+\eta_*^2)\right] + \frac{\tilde{z}_*}{Re_i} \qquad (C.5)$$

while in the particular case of $\eta_* \to 0$ one gets immediately from (C.3)

$$\frac{\hat{Z}_F}{Re_L} = \frac{3}{8}\,\frac{1-W_F}{\gamma_F-1}\left[\frac{1}{W_F} - 1 + \frac{\gamma_F-1}{\gamma_F-W_F}\,\ln\frac{\gamma_F}{W_F}\right] \tag{20}$$

TABLE 1

Consequences of the Shvab-Zeldovich Technique

	Inside the Flame $W > W_F$	Outside the Flame $W < W_F$
y_1	$\frac{W - W_F}{1 - W_F}$	0
y_2	0	$\frac{1}{f}\frac{W_F - W}{1 - W_F}$
y_3	$\frac{1-W}{1-W_F}(1+f)W_F$	$\frac{1+f}{f}W$
τ	$\frac{1-W}{1-W_F}$	$\frac{W}{W_F}$
ν	$1+(\nu_F-1)\frac{1-W}{1-W_F}$	$1+(\nu_F-1)\frac{W}{W_F}$

TABLE 2

Relevant Properties of Hydrogen, Some Hydrocarbons, and Air

at N. T. P.

	M	Sc	Pr	μ/ρ cm^2/sec	ν_F	W_F
Hydrogen	2	1.53	0.71	1.059	7.81	0.028
Methane	16	0.77	0.72	0.1648	7.25	0.055
Ethylene	28	0.56	0.90	0.0858	7.58	0.064
Propylene	42	0.37	0.74	0.0437	7.45	0.064
Air	29	—	0.71	0.259	—	—

FIGURE CAPTIONS

Fig. 1 Planar Flame Shapes - XBL 818-11257

Fig. 2 Dependence of Flame Length on - XBL 818-11265

Fig. 3 Axi-Symmetric Flame Shapes - XBL 818-11259

Fig. 4 Normalized Axi-Symmetric Velocity Profiles for the case of $\gamma_F = 7$, $W'_F = 0.06$. - XBL 818-11260

Fig. 5 Flame Structure for the case of $\gamma_F = 7$, $W'_F = 0.06$. - XBL 818-11261

Fig. 6 Flame Lengths Data of Refs. 12 and 13 - XBL 818-11258

Fig. 7 Flame Widths Data of Refs. 12 and 13 - XBL 818-11262

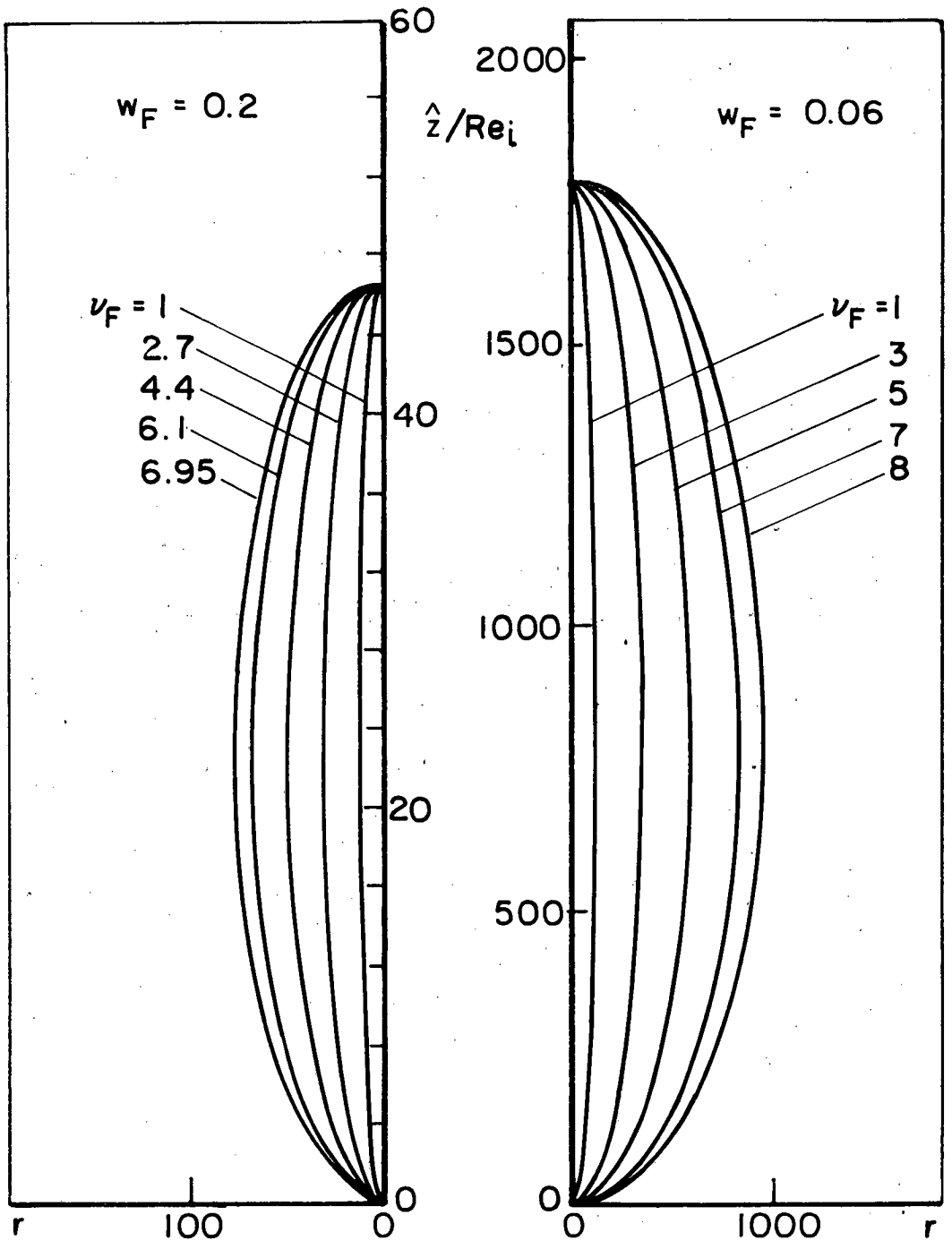

Fig. 1

XBL 818-11257

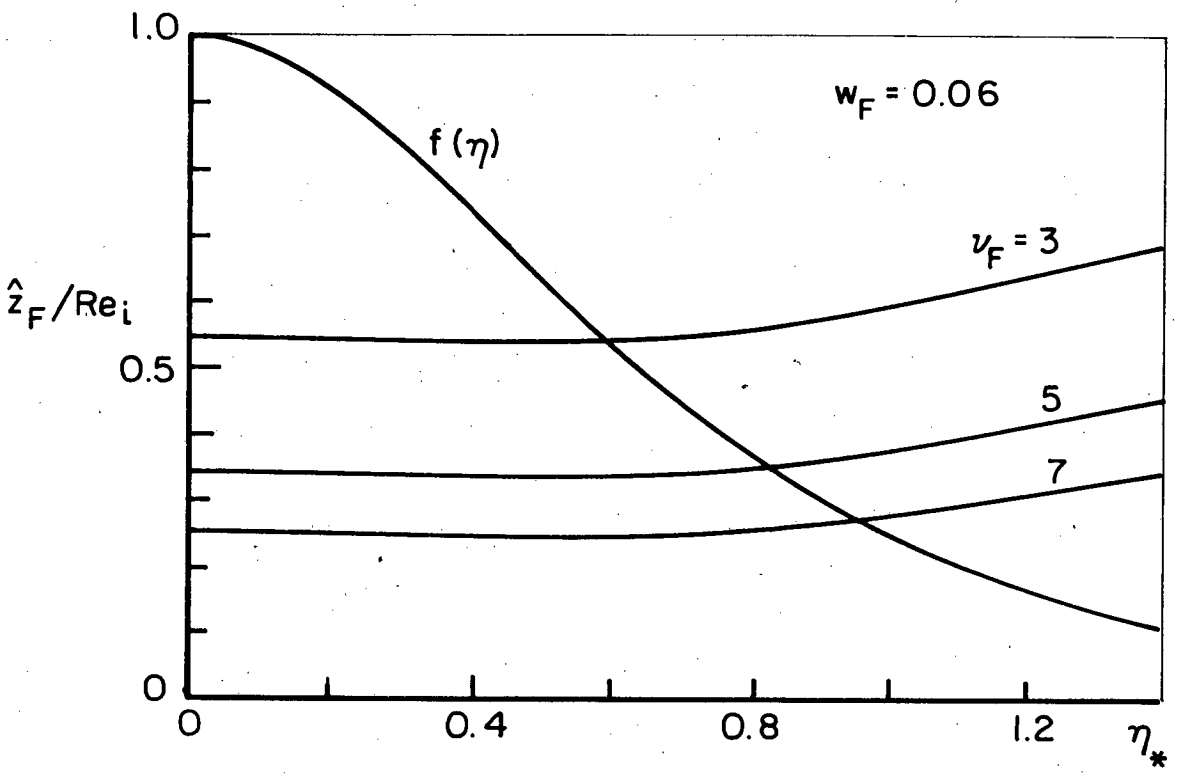

Fig. 2

XBL 818-11265

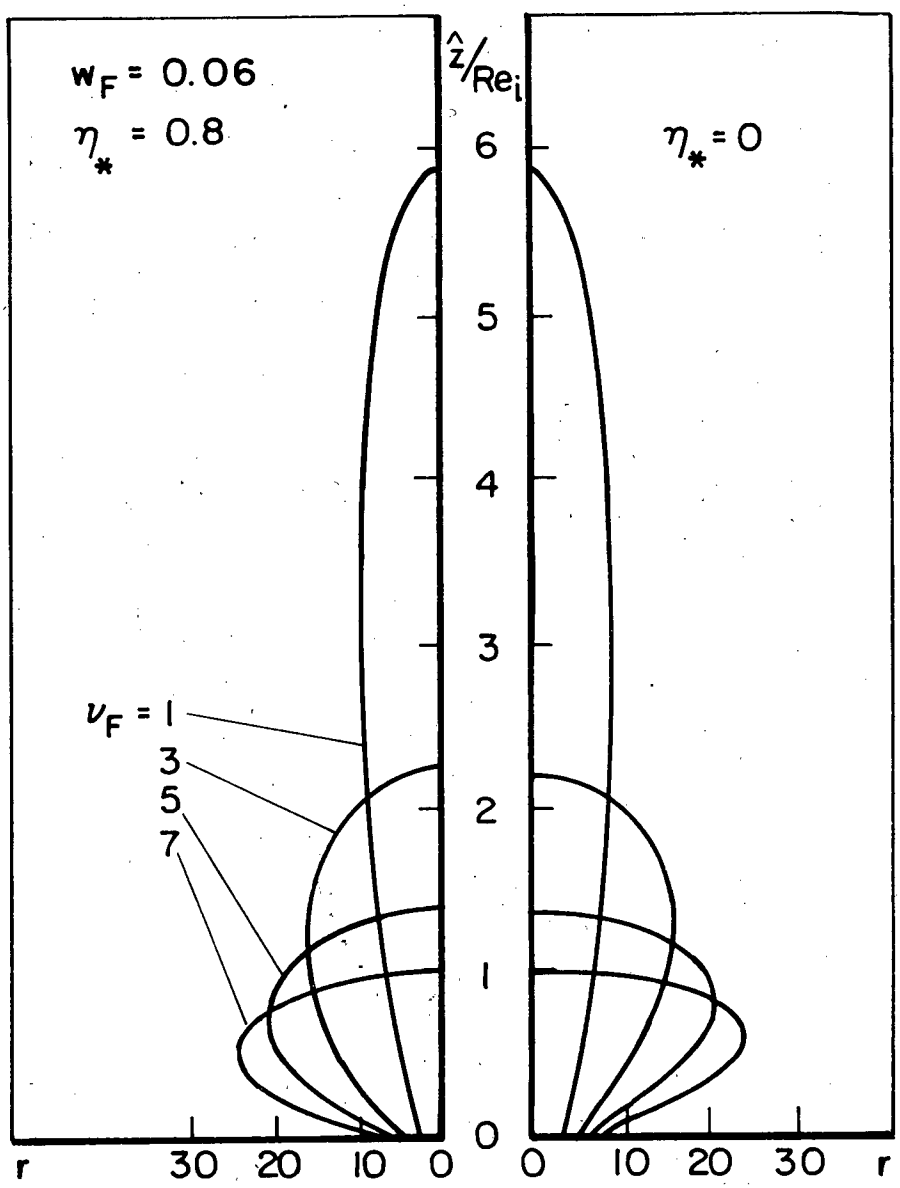

Fig. 3

XBL 818-11259

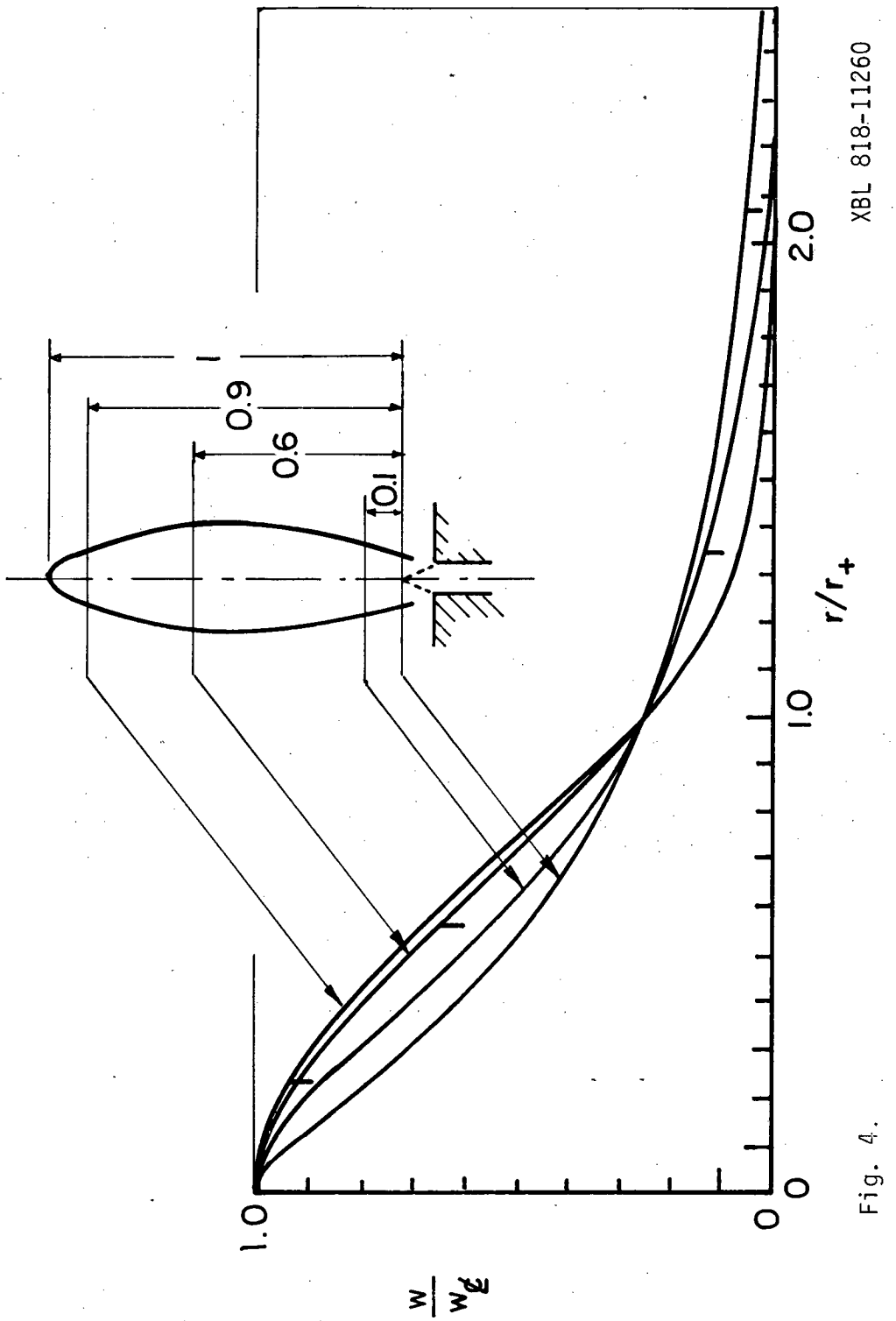

XBL 818-11260

Fig. 4.

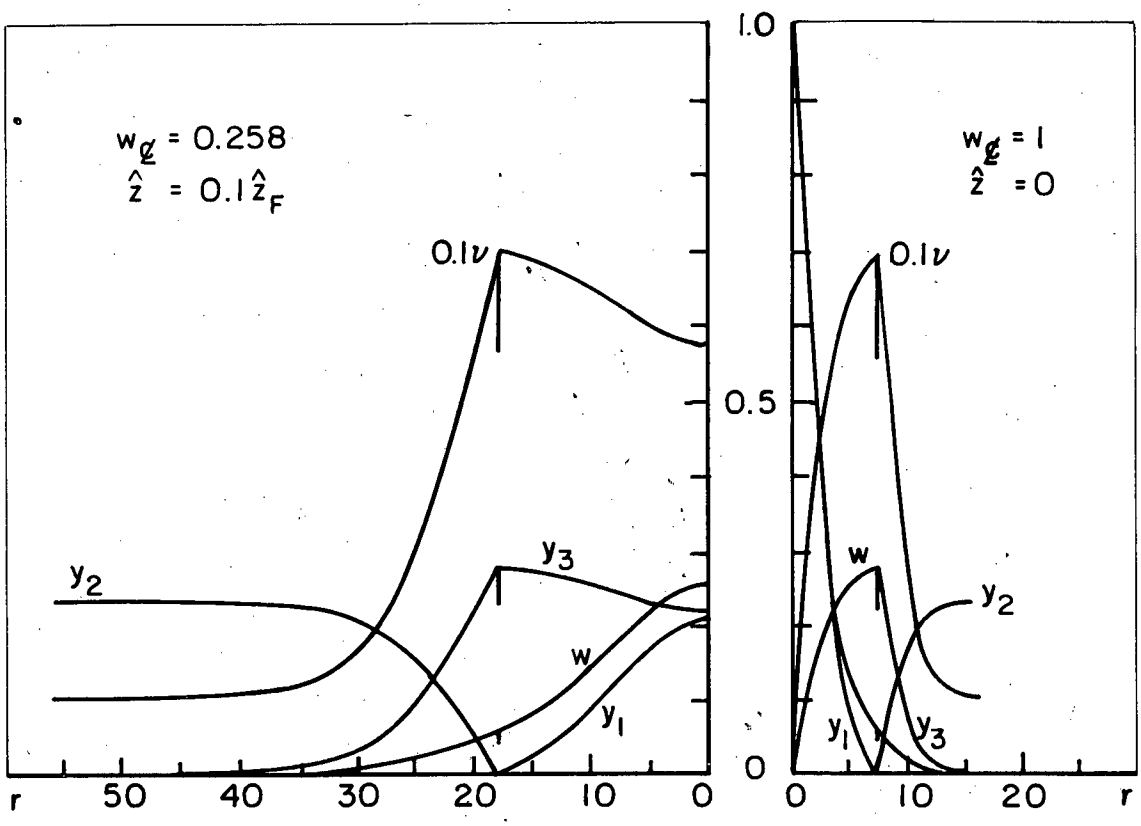

Fig. 5

XBL 818-11261

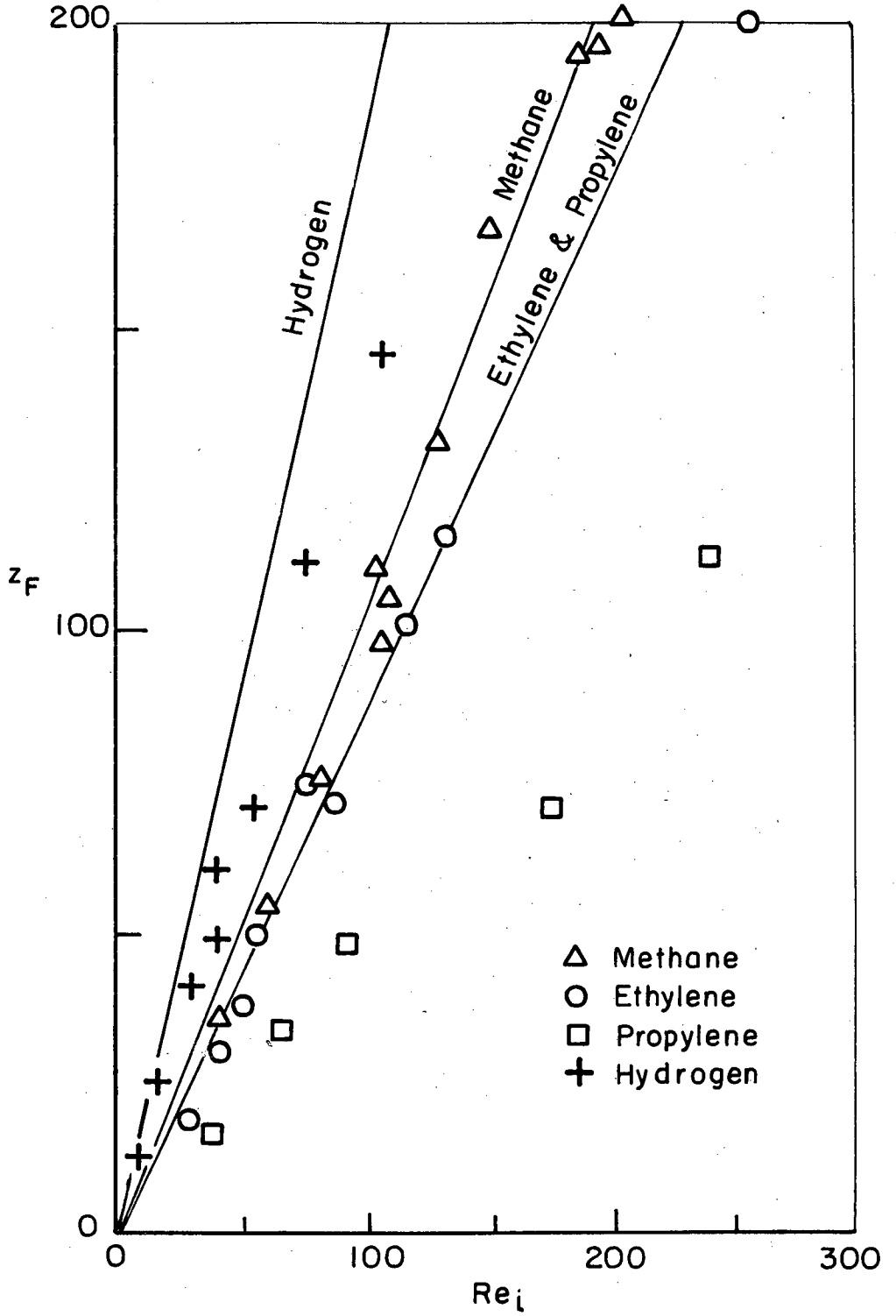

Fig. 6

XBL 818-11258

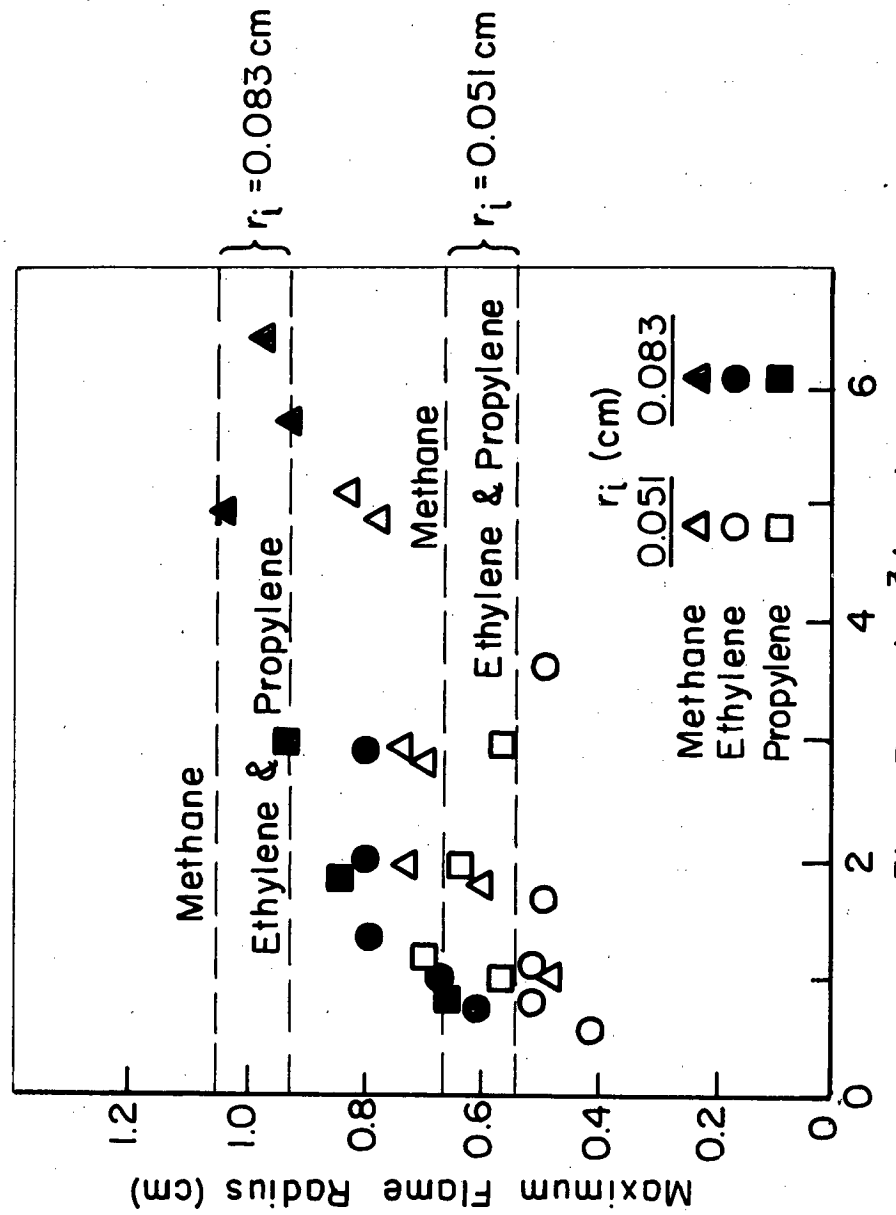

XBL 818-11262

Fig. 7

TECHNICAL INFORMATION DEPARTMENT
LAWRENCE BERKELEY LABORATORY
UNIVERSITY OF CALIFORNIA
BERKELEY, CALIFORNIA 94720